

## Signal Analysis of Vibration Measurements for Condition Monitoring of Bearings

<sup>1</sup>Jalel Chebil, <sup>2</sup>Meftah Hrairi, <sup>3</sup>Nazih Abushikhah

<sup>1</sup>Electrical and Computer Engineering Department

<sup>2</sup>Mechanical Engineering Department International Islamic University Malaysia Kuala Lumpur, Malaysia

<sup>3</sup>Communication and Electronics Engineering Department Faculty of Engineering Amman Private University Amman, Jordan

---

**Abstract:** Rotating machinery is a common class of machinery in industry. The root cause of faults in rotating machinery is often faulty rolling element bearings. These rolling element bearings wear out easily due to the metal-metal contacts and create faults in the outer race, inner race, or balls. This study compares several techniques used for monitoring bearing condition. These techniques are based on the processing of vibrational data in the time-domain, frequency-domain, or time-frequency-domain. It was found that the discrete wavelet transform which is based on time-frequency analysis produces the best results.

**Key words:** rolling element bearings; inner and outer race faults; vibration signals; signals processing; wavelet.

---

### INTRODUCTION

Bearings are of paramount importance to almost all forms of rotating machinery, and are among the most common machine elements. The failures of bearing without warning will result in catastrophic consequences in many situations, such as in helicopters, transportation vehicles, etc. Most of the current maintenance procedures include periodic visual inspections and replacement of the components at fixed time intervals. The application of structural health monitoring techniques, which provides in-service assessment and prediction of the structural component health, will clearly result in a much lower operational cost, early detection of faults of small magnitude, accurate assessment of current fault or defect size, and accurate prediction of fault progression Zhang, *et al.*, (2005).

All bearings, even those in perfect condition, produce noise as the elements roll over the raceways and rub against the internal cage and flanges. This noise is generated at high frequency and low amplitude. The bearing housing amplifies the noise to a point where a sensitive accelerometer can hear them. By careful detection and filtering, the noise signal can be amplified and represented as a frequency series in real-time. This constitutes the basis of roller bearing vibration measurement which is one of the major condition monitoring tools in regular use. By analyzing the vibration signals emitted from a rolling bearing, it is possible to tell its condition and the likelihood of imminent failure.

The structure of this paper is as follows. In Section 2, a description of the typical faults of the bearing is presented while the basic concepts in wavelet analysis are explained in Section 3. The data used for monitoring and diagnosis is described in Section 4, whereas the detailed fault diagnosis procedure based on wavelet analysis is discussed in Section 5. The last section concludes the paper.

#### **Bearing Faults:**

Most bearing faults occur with the rolling elements, cage, or raceways. Thus, the different faults occurring in a rolling-element bearing can be classified according to the damaged element as: (1) outer raceway defect; (2) inner raceway defect; (3) ball defect. The fault is assumed to be modeled as a small hole created from a missing piece of material on the corresponding element. The frequency of the fault has a direct relationship with the geometry of the bearing and the relative speed of each individual raceway.

The resonant frequencies can be calculated theoretically. Each bearing element has a characteristic rotational frequency. With a defect on a particular bearing element, an increase in the vibration energy at this element rotational frequency may occur. This defect frequency can be calculated from the geometry of the

bearing and element rotational speed. Fig. 1 shows the bearing and the contact angle.

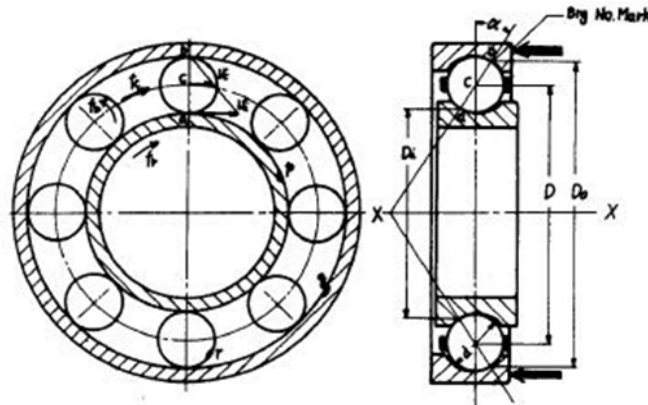


**Fig. 1:** Motion of ball bearing and contact angle Igarashi and Kato, (1985).

*Frequencies associated with defective bearings are as follows:*

$$ORF \text{ frequency} = \frac{n}{2} \left( \frac{Ns}{60} \right) \left( 1 - \frac{d}{D} \cos \alpha \right) \quad (1)$$

$$IRF \text{ frequency} = \frac{n}{2} \left( \frac{Ns}{60} \right) \left( 1 + \frac{d}{D} \cos \alpha \right) \quad (2)$$

$$BF \text{ frequency} = \frac{D}{d} \left( \frac{Ns}{60} \right) \left( 1 - \frac{d^2}{D^2} \cos^2 \alpha \right) \quad (3)$$

where,

- $N_s$  = the rpm of the shaft
- $d$  = the mean diameter of the rolling elements
- $D$  = the pitch diameter of the bearing
- $n$  = the number of rolling elements
- $\alpha$  = the contact angle

A roller bearing progresses through four stages to failure. Vibration analysis permits the monitoring of the bearing's progression through each stage and to estimate when failure will actually occur. In the case of a raceway failure these would be the four progressive stages.

The bearing is new and has no defects. This is the time to record its frequency 'signature' and normal operating acceleration and velocity values.

If examined at this stage there would be no visible defects. However under the surface of the raceway sub-surface defects have started. The frequency signature has changed, the overall base level noise has risen and the velocity spectrum (graph) has risen higher.

At this point the raceway shows visible signs of surface failure. The extent of the failure increases and grows with more metal coming off in minute sheets (delaminating). The velocity spectrum is much higher and much more background noise has developed. Within the background noise particular frequencies start to stand out (side bands) and indicate failure is fast approaching.

If the bearing is still in service everyone knows it is time to change it out because they can hear it. More vibration frequencies appear and more velocity side bands develop. Readings start to indicate amplitude changes and the noise moves into the range of human hearing.

Bearing vibration analysis can detect lubrication failures, misalignment, out of tolerance running, rubbing, improper gear teeth meshing, out of balance, bent shafts, loose components, worn parts, faulty couplings, improper operating conditions (like pump cavitation) and deflecting support structures. However to be able to analyze the presence of these type of problems requires a highly skilled person with much experience and exposure to bearing vibration signatures at various stages of failure.

**Common methods used in the detection and diagnosis of faults in ball bearing:**

A wide variety of techniques, using various algorithms were developed for the detection and diagnosis of faults in rolling element bearings, have been introduced to inspect raw vibration signals. These algorithms can be classified into time domain, frequency domain, time-frequency domain, higher order spectral analysis, neural-network and model based techniques. This study will mainly investigate techniques based on time domain, frequency domain and time-frequency domain.

Time domain approaches are based on the analysis of the vibration data as a function of time. The principal advantage of this type of analysis is that no data is lost prior to inspection. However, the disadvantage is that there is often too much data for easy and clear fault diagnosis Patil *et al.*, (2008). Features are extracted from the time-domain representation of vibration signals such as peak value, mean, root-mean-square (RMS), kurtosis, crest factor, impulse factor, shape factor, and clearance factor.

$$\text{Peak Value, Pv} = \frac{1}{2} [\max(x_i) - \min(x_i)] \tag{4}$$

$$\text{Mean} = \mu = \frac{1}{N} \sum_{i=1}^N x_i \tag{5}$$

$$\sigma = \sqrt{\left(\frac{1}{N} \sum_{i=1}^N (x_i - \mu)^2\right)} \tag{6}$$

$$\text{RMS Value} = \sqrt{\frac{1}{N} \sum_{i=1}^N (x_i)^2} \tag{7}$$

$$\text{Crest factor, Crf} = \frac{\text{Peak value}}{\text{RMS Value}} \tag{8}$$

$$\text{Clearance factor, Clf} = \frac{\text{Peak Value}}{\left[\frac{1}{N} \sum_{i=1}^N \sqrt{|x_i|}\right]^2} \tag{9}$$

$$\text{Impulse factor, Imf} = \frac{\text{Peak Value}}{\frac{1}{N} \sum_{i=1}^N |x_i|} \tag{10}$$

$$\text{Shape factor, shf} = \frac{\text{RMS Value}}{\frac{1}{N} \sum_{i=1}^N |x_i|} \tag{11}$$

The frequency domain refers to the display or analysis of the vibration data based on the frequency. The most basic and well-known method in this group is spectral analysis based on the discrete Fourier transform (DFT). It has become very popular since the birth of the fast Fourier transform (FFT) algorithm. The power spectrum reveals how energy is distributed over frequencies and therefore is very useful in identifying periodic phenomena and determining their strength. Because a large number of forcing functions in rotating machines are proportional to a fundamental frequency such as the rotating frequency, spectra sometimes are plotted against multiples (integer or fractional) of rotational speed, which are called orders. The principal advantage of the method is that the repetitive nature of the vibration signals is clearly displaced as peaks in the frequency spectrum at the frequency where the repetition takes place. The interaction of the defect in the rolling element bearings produces pulses of very short duration, whereas the defect strikes the rotation motion of the system. These pulses excite the natural frequency of the bearing elements, resulting in the increase in the vibration energy at these high frequencies Budynas and Keith Nisbett, *et al.*, (2008).

Time-frequency domain techniques use both time and frequency domain information allowing for the investigation of transient features. A number of time-frequency domain techniques have been proposed

including the short time Fourier transform, the Wigner-Ville distribution, and the wavelet transform. This paper focuses only on the use of discrete wavelet analysis in the detection and diagnosis of ball bearing faults. The discrete wavelet transform offers simultaneous interpretation of the signal in both time and frequency domain which allows local, transient or intermittent components to be exposed. Such components are often obscured due to averaging inherent within spectral-only methods such as the Fourier transform. The discrete wavelet transform (DWT) employs a dyadic grid and orthonormal wavelet basis functions and exhibits zero redundancy. The DWT computes the wavelet coefficients at discrete intervals (integer power of two) of time and scales Mertins, (1999). The computed DWT coefficients can be used to form a set of features that unambiguously characterize different types of signals. The dilation function of the DWT can be represented as a tree of low and high pass filters, with each step transforming the low pass filter into further lower and higher frequency components. The original signal is successively decomposed into components of lower resolution, while the high frequency components are not analyzed any further. The low-frequency components of the signal are called approximations, while the high-frequency components are called details Chebil *et al.*, (2009). The DWT is defined as Tzanetakis *et al.*, (2001).

$$W(j, k) = \sum_j \sum_k x(k) 2^{-j/2} \psi(2^{-j} n - k) \quad (12)$$

where  $x(k)$  is the signal,  $y(t)$  is a time function with finite energy and fast decay and it is called the mother wavelet.

#### **Experimental Data:**

The investigation in this paper is entirely based on the vibration data obtained from the Case Western Reserve University Bearing Data Centre website Loparo, (2009). As shown in Fig. 2, the data was collected from an accelerometer mounted on the housing of an induction motor system coupled to a load that can be varied within the operating range of the motor. The data collection was done for the drive-end bearing.

Data was gathered for four different conditions: (i) normal (N); (ii) inner race fault (IRF); (iii) outer race fault (ORF); (iv) ball fault (BF). Faults were introduced into the drive end bearing by using electro-discharge machining. For inner race and ball fault cases, the size of the fault is 0.1778, 0.3556, and 0.5334 mm. For outer race fault case, the size of the fault is either 0.1778 or 0.5334 mm. The data is sampled at a rate of 12 kHz and the duration of each vibration signal was 10 seconds. All the experiments were repeated for four different load conditions: 0, 1, 2 and 3 horse power (HP).

The experimental data consisted of four vibration signals for the normal condition (collected from a single bearing) and 12 vibration signals for each of the three fault conditions. The data in each category (normal, IRF, BF and ORF) is segmented into 58 sets with each set having 2048 samples. The reason for selecting 2048 samples is to get nearly 6 complete rotations since the motor speed is ranging from 1730 to 1797 rotation per minute. Hence there are 232 data sets from the normal condition, and 696 data sets from each of the faulty conditions. Before any processing, the data has been cleaned from any associated noise by passing through a high pass filter.

## **RESULTS AND DISCUSSIONS**

As mentioned earlier, this study investigates the performance of the various existing techniques in the detection and diagnosis of faults in ball bearing elements. We will first discuss the time-domain approaches, followed by methods based on frequency and time-frequency domains methods.

#### **Methods Based on Time-Domain Analysis:**

The first part of this study will investigate the performance of the existing time domain techniques when applied to the data sets discussed earlier. Three data sets from each type are used for training in order to select the appropriate threshold values for the methods based on peak value, root-mean-square (RMS), mean, standard deviation (STD), kurtosis, crest factor (Crf), clearance factor (Clf), impulse factor (Imf) and shape factor (Shf). The rest of the data is used for testing. Fig. 3 shows the results of the test when different loads are considered with the same fault size, whereas Fig. 4 displays the results for any load and for any fault size. Three of the nine features produce good detection of incipient faults which are peak value, RMS and Clf for the first test. However, when all the data sets are considered, the best performance is obtained by the peak value followed by Clf and RMS. The highest accuracy obtained is less than 70%, this indicates the shortcoming of this approach.

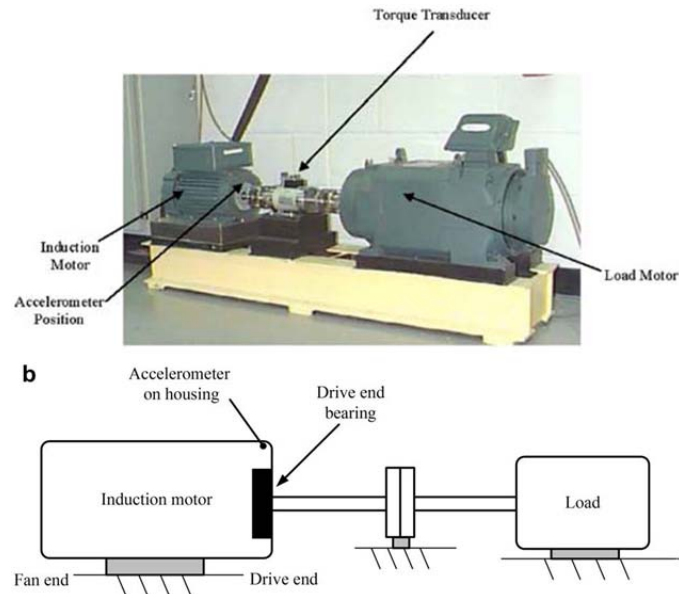


**Fig. 2:** (a) The bearing test rig; (b) the schematic description of the test rig. Huang *et al.*, (2010)

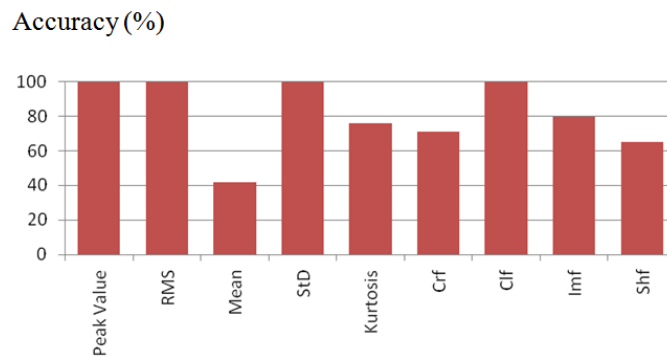


**Fig. 3:** Accuracy of the features used in time-domain for different loads but same size fault

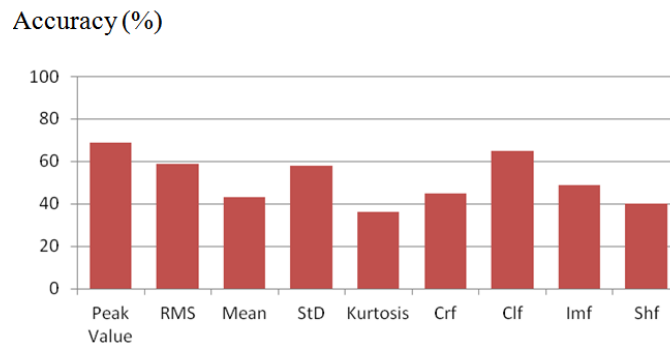


**Fig. 4:** Accuracy of the features used in time-domain for different loads and for various size faults

**Methods Based on Frequency Analysis:**

For the frequency domain analysis, Fig. 5 shows the power spectrums of some sampled data for normal and three faulty conditions (IRF, BF and ORF). For normal conditions, the energy contents of the signal are significantly below 2 kHz. However, faulty signals have additional significant components at higher frequencies ranging from 2 kHz to 6 kHz. These components should be very important in the detection of faulty bearings and the diagnosis of the fault size and fault location. In the frequency-domain approach, two features were tested, namely resonant frequency and signal energy.

The first approach is based on the mechanical phenomenon of resonance. For a normal behavior, the mechanical system is built to avoid resonance. But when there is a fault in the bearing, the resonant frequencies are likely to appear in the spectrum as peaks in high frequencies. The location of the frequency peaks can be used to distinguish between normal and abnormal behaviors. In this approach, the locations of the three first dominant frequency peaks obtained from the signal spectrums are used as features to discriminate between healthy and faulty behaviors. This criterion was found to be 100% efficient in the detection of the faulty ball bearing elements Chebil *et al.*, (2009). However, this criterion is not sufficient to find the location of the fault. The knowledge of the estimated resonant frequencies can be very useful in improving this approach. Analytically, the resonant frequencies can be estimated by using equations (1) to (3). Table I displays the calculated frequencies for the ball bearing elements used in the experiment conducted by the Case Western Reserve University Bearing Data Centre for a load of 1 HP.

The spectrums of sample data sets with IRF fault of various sizes were analyzed. It is observed that in many cases the differences between the frequencies of the three highest peaks tend to be multiples of the resonant frequency of 160 Hz. The same applies for the ORF and BF faulty signals. However, there are other frequency components which are present due to the motor speed. These components are located at multiples of the fundamental frequency which depend on the motor speed, which is about 30 Hz. This will cause many errors in using this approach. For this reason, it was difficult to devise a technique that automatically detects these resonant frequencies with good accuracy.

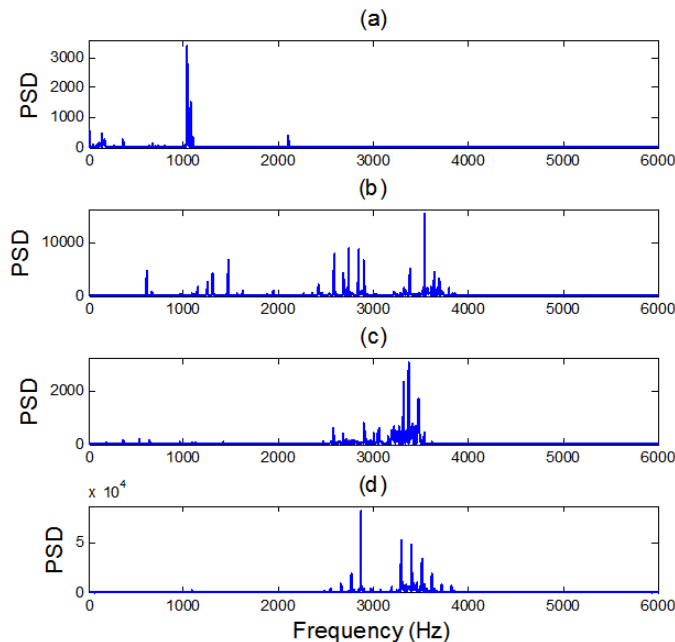


**Fig. 5:** Graph of the power spectrum for sample of vibration data for (a) normal, (b) IRF, (c) BF, and (d) ORF

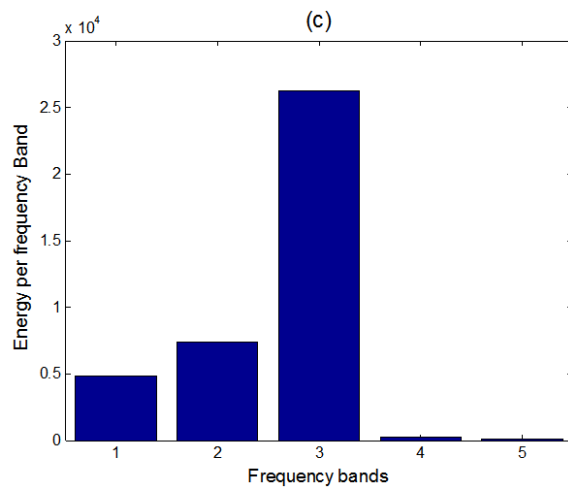
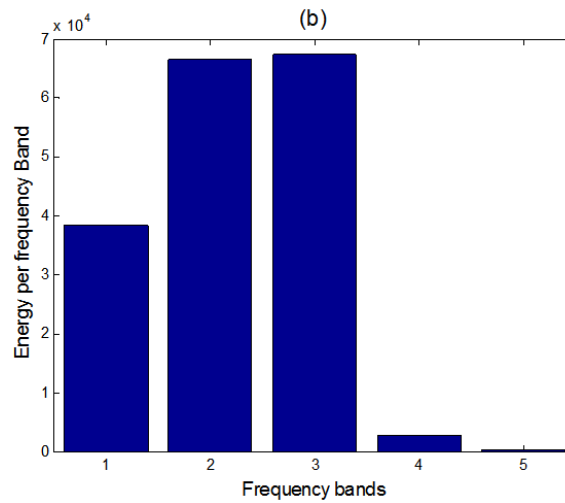
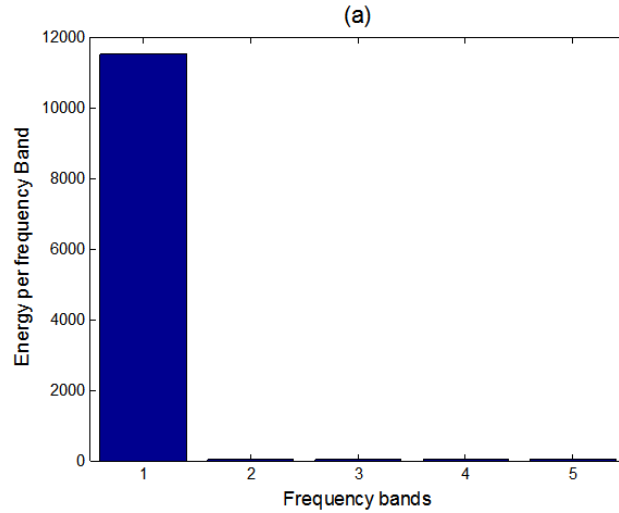
**Table 1:** Resonant Frequencies for Faulty Ball Bearing Elements for a Load of 1 Hp.

	Inner race fault	Ball fault	Outer race fault
Resonant frequency (Hz)	160	139	106

The second approach is based on the fact that cracks are translated into transient and high frequency phenomena in the vibration signal. Consequently, the abnormal behavior can be detected by analyzing the percentage of energy contained in high frequencies. It was found that when this approach is applied to the available data, the percentage of energy contained in the higher frequencies is large if the bearing is faulty, and small if the bearing is healthy.

Fig. 6 shows sample results of the average energy contained in the frequency sub-bands 1, 2, 3, and 4 for vibration data for the normal and abnormal bearings. The results demonstrate that the average energy in the first band is always the highest if the bearing is normal, while it will be highest in other frequency bands if the bearing has defects. From these experiments, we could efficiently distinguish with an accuracy of 100% between normal and faulty ball bearing behaviors by comparing the average energy of each sub-band. For the diagnosis of the fault location, an algorithm was devised by computing the four energy bands that uses

threshold values that were obtained from the training data. However, when the algorithm is tested with the remaining data, the accuracy obtained is only 77.8%. Altering the threshold values did not produce much improvement. The result is lower than expected and there is need to explore the time-frequency domain technique which will be discussed next.



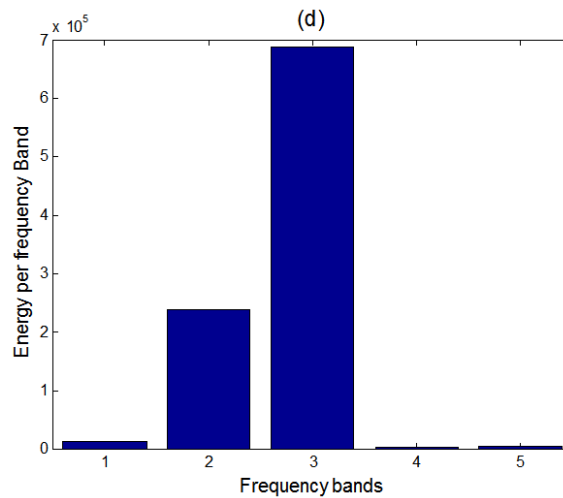


**Fig. 6:** Average energy contained in the frequency sub-bands: band1 [0-1500], band2 [1500-3000], band3 [3000-4500], and band4 [4500-6000] for vibration data for rolling element bearing with (a) no fault, (b) IRF, (c) BF, and (d) ORF.

**Method based on time-frequency analysis:**

In this approach, two features were investigated namely the peak and RMS values using the DWT. The data is first decomposed by using a second level DWT with a Daubechies mother wavelet (Db4). Based on the training data, two observations were noted. First, the peak and RMS values of the second level approximation is always much higher than the details of the first and second level decomposition for normal ball bearing elements. This characteristic is used as a criterion to distinguish between normal and faulty data. Second, it is possible to differentiate between the three types of fault by allocating specific ranges for the IRF, BF, and ORF faulty signals based on the peak or RMS values of the details of the first and second level decompositions. Using these two criteria, it was found that the accuracy is 85.1% if the method is based on the peak value feature, and it is 89.3% if the method uses the RMS feature. Table II shows the best resulting accuracy obtained from approaches based on time, frequency, and time-frequency using specific features. It is clear that DWT, which is a time-frequency approach, outperforms the other methods. The best result was obtained using the RMS feature. In addition, the DWT approach is more flexible and can be enhanced if a higher decomposition level is explored.

**Table 2:** Accuracy of the important results obtained using time, frequency and DWT approaches.

	Time- Peak	Time- RMS	Time- Clf	Frequency Bands	DWT- Peak	DWT- RMS
Accuracy(%)	69.0	59.0	65.0	77.8	85.1	89.3

**Conclusion:**

This study compares the performance of various approaches used in the detection and diagnosis of ball bearing elements using vibrational data obtained from the Case Western Reserve University Bearing Data Centre website. It was found that the approaches based on DWT and using the RMS feature outperforms other techniques.

**ACKNOWLEDGMENT**

The authors gratefully thank Mr Hairul Anuar Hajali and Mr. Rafizan bin Tusiman for their assistance.

**REFERENCES**

Budynas, R.G., J. Keith Nisbett, 2008. Shigley’s Mechanical Engineering Design; McGraw-Hill; Singapore.  
 Chebil, J., G. Noel, M. Mesbah, M. Deriche, 2009. “Wavelet Decomposition for the Detection and Diagnosis of Faults in Rolling Element Bearings”, Jordan Journal of Mechanical and Industrial Engineering, 3(4): 260-26.

Huang, Y., C. Liu, X.F. Zha, Y. Li, 2010. "A lean model for performance assessment of machinery using second generation wavelet packet transform and Fisher criterion," *Expert Systems with Applications*, 37: 3815-3822.

Igarashi, T., K. Kato, 1985. "Studies on the Vibration and Sound of Defective Rolling Bearings," 3rd Report: Vibration of Ball Bearings With Multiple Defects, *Bull. JSME*, 28(237): 492-499.

Loparo, K.A., 2009. Bearing data center, Case Western Reserve University. <http://www.eecs.case.edu/laboratory/bearing/download.htm>, Retrieved.

Mertins, A., 1999. "Signal Analysis: Wavelets, Filter Banks, Time-Frequency Transforms and Applications", John Wiley & Sons Ltd.

Patil, M.S., J. Mathew, P.K. RajendraKumar, 2008. "Bearing Signature Analysis as a Medium for Fault Detection: A Review". *Journal of Tribology*, 130(1): 014001.

Tzanetakis, G., G. Essl and P. Cook, 2001. "Audio Analysis using the Discrete Wavelet Transform", *Proc. Conf. in Acoustics and Music Theory Applications*.

Zhang, X., R. Xu, C. Kwan, S.Y. Liang, Q. Xie and L. Haynes, 2005. "An integrated approach to bearing fault diagnostics and prognostics," *American Control Conference*, Portland, OR, USA, pp: 2750-2755.